

# Numerical Simulation of TNT-Al Explosives in Explosion Chamber

F. Togashi\*, J. D. Baum\*, O. A. Soto\*, R. Löhner\*\*, and F. Zhang\*\*\*  
Corresponding author: fumiya.togashi@saic.com

\* SAIC, USA

\*\* George Mason University, USA.

\*\*\* DRDC Suffield, Canada

**Abstract:** The Numerical modeling of burning particles, initiated from a heavily aluminized High Explosive (HE) is being investigated. Reactive multiphase flows must be modeled to properly account for variable-size aluminum particles burning behind the blast wave. The governing equations also include models for solid evaporation and chemical reactions. The final paper will present comparison of experimental data and computational results of mixed TNT-Al detonation and burning in a closed chamber.

*Keywords:* Computational Fluid Dynamics, Blast Wave, Afterburning, Multi-phase Flow

## 1 Introduction

Aluminum particles are often mixed into solid propellants or explosives to enhance energy release, which can burn in the high pressure and high temperature condition behind the detonation wave. The aluminum particle reaction is very complicated because they react with detonation products at first such as  $H_2O$ ,  $CO_2$ , *etc.*, and then start reacting with ambient air. Their evaporation mechanism and slower reaction time also have to be considered. Those issues are bottleneck of the numerical simulation of aluminized HEs. Especially when HEs are cased, the computations are much more difficult because of the case breaking, melting, reacting, and so on. However, an accurate numerical analysis of heavily aluminized HEs is critical to ensure its safe usage because of the difficulty of understanding the experimental results.

There are various Equation of State (EOS) to compute the blast wave initiated from HEs. One of the famous EOS is the Jones-Wilkins-Lee (JWL) model [1]. This model is a simple and robust equation which shows good agreement with the incident pressure peak value and its time of arrival (TOA). However this model does not guarantee the accuracy of the longterm blast evolution or reverberation under the condition of confined facilities. When the blast phenomenon occurs in a confined situation and the HE is fuel rich, the afterburn of detonation species should be considered. Generally Miller model [2] is used to treat an afterburn effect of HEs. Authors reported the afterburning effect of long-duration blast wave evolution in confined facility using the JWL-Miller model [3]. The results agreed well with experimental data. This methodology, however, may only be applicable to larger sizes of confined surroundings and smaller sizes of burnable particles because this methodology releases the afterburning energy via the function of the pressure and neither considers the chemical reaction nor the particle evaporation. The multi-phase flow with the chemical reaction model is required for post-detonation combustion in a relatively small room or a cased HE.

Ripley *et al.*, Kim *et al.* and Balakrishnan *et al.* have reported numerical simulations of the aluminum

afterburning behind TNT detonations [4, 5, and 6]. They applied the Khasainov's empirical quasi-steady law [7] for aluminum evaporation in a multi-phase flow and used a simple chemical reaction model, i.e., infinite chemical reaction rates [8, 9], to the afterburning behind the blast wave. Nobel-Abel EOS [10] was used to model the blast wave propagation. TNT ( $C_7H_5N_3O_6$ ) was assumed to decompose to 4 species:  $N_2$ ,  $H_2O$ ,  $CO$ , and  $C$  as follows:

$C_7H_5N_3O_6 \rightarrow 1.5N_2 + 2.5H_2O + 3.5CO + 3.5C$  [11]. These models chose to ignore the presence and energy release of oxidizers, and binders. Establishing the numerical modeling to handle such HEs, whose composition includes oxidizers and binders, is very significant to practical engineering. The purpose of this research is to develop numerical models having the capability of treating the burning of multiple-sized aluminum particles which are mixed into the various types of HEs.

## 2 Governing Equations and Chemical Reaction Modeling

The governing equations for the multi-phase flow are as follows:

$$\frac{\partial \mathbf{Q}}{\partial t} + \frac{\partial \mathbf{E}}{\partial x} = \mathbf{S}_1 + \mathbf{S}_2 + \mathbf{S}_3 \quad (1)$$

$$\mathbf{Q} = \begin{bmatrix} \rho_{gk} \\ \rho_g \\ \rho_g u_g \\ e_g \\ \phi_s \rho_s \\ \phi_s \rho_s u_s \\ \phi_s \rho_s E_s \\ N_p \end{bmatrix}, \mathbf{E} = \begin{bmatrix} \rho_{gk} u_g \\ \rho_g u_g \\ \rho_g u_g^2 + P \\ (e_g + P)u_g \\ \phi_s \rho_s u_s \\ \phi_s \rho_s u_s^2 \\ \phi_s \rho_s E_s u_s \\ N_p u_s \end{bmatrix},$$

$$\mathbf{S}_1 = \begin{bmatrix} \frac{1}{1-\phi_s} \xi_k \Delta c (1 - \frac{\rho_g}{\rho_s}) + \dot{\omega}_k \\ \frac{1}{1-\phi_s} \Delta c (1 - \frac{\rho_g}{\rho_s}) \\ \frac{1}{1-\phi_s} \Delta c (u_s - u_g \frac{\rho_g}{\rho_s}) \\ \frac{1}{1-\phi_s} \Delta c (E_s - E_g \frac{\rho_g}{\rho_s}) \\ -\Delta c \\ -\Delta c u_s \\ -\Delta c E_s \\ 0 \end{bmatrix}, \mathbf{S}_2 = \begin{bmatrix} 0 \\ 0 \\ \frac{1}{1-\phi_s} (\frac{\Delta c}{2} - \delta)(u_g - u_s) \\ \frac{1}{1-\phi_s} (\frac{\Delta c}{2} - \delta)(U_g - U_s)U_s \\ 0 \\ -(\frac{\Delta c}{2} - \delta)(u_g - u_s) \\ -(\frac{\Delta c}{2} - \delta)(U_g - U_s)U_s \\ 0 \end{bmatrix}, \mathbf{S}_3 = \begin{bmatrix} 0 \\ 0 \\ 0 \\ -\frac{1}{1-\phi_s} h(T_g - T_s) \\ 0 \\ 0 \\ h(T_g - T_s) \\ 0 \end{bmatrix}$$

(2)

where the three added source term vectors are related to the mass transfer ( $\mathbf{S}_1$ ), momentum ( $\mathbf{S}_2$ ), and energy ( $\mathbf{S}_3$ ) between the phases. The first row of the governing equations denotes chemical reaction handling  $k$ -th reactions. Second to 4<sup>th</sup> rows are the governing equations for gas-phase, and 5<sup>th</sup> to 8<sup>th</sup>

rows are the governing equations for solid-phase. Subscript  $g$  denotes gas-phase, subscript  $s$  denotes solid-phase, and subscript  $k$  denotes  $k$ -th species respectively.  $\phi_s$  denotes the solid-phase volume fraction, and  $N_p$  denotes particle number density. The terms  $U_g$  and  $U_s$  denote velocity vectors for gas and solid-phase. The terms  $T_g, T_s$  also denote the temperatures of the gas and solid respectively. The term  $\xi_k$  denotes the  $k$ -th species contribution factor. The term  $\dot{\omega}_k$  denotes the  $k$ -th species source due to the homogeneous chemical reactions. The terms:  $\delta, d$ , and  $h$  denote drag force factor, average particle diameter, and energy exchange factor between the phases. They can be written as follows:

$$\delta = \frac{3}{4}(\phi_s / d)C_x \rho_g |u_g - u_s| \quad (3)$$

where  $C_x$  is the drag force coefficient obtained from a formula proposed by Hendrson [12].

$$d = (6\phi_s / \pi N_p)^{1/3} \quad (4)$$

$$h = 6\phi_s (Nu \lambda_g / d^2) \quad (5)$$

Nu is a Nusselt number calculated from equations derived by Carlson and Hoglund [13].

$$Nu = \frac{2 + 0.459 Re^{0.55} Pr^{0.33}}{1 + 3.42 \frac{Ma}{Re Pr} (2 + 0.459 Re^{0.55} Pr^{0.33})} \quad (6)$$

where Pr is the Prandtl number is defined as follows:

$$Pr = \frac{C_{pg} \mu_g}{\lambda_g} \quad (7)$$

$C_{pg}$  is the gas-phase specific heat at constant pressure,  $\mu_g$  is the gas-phase viscosity, and  $\lambda_g$  is thermal conductivity.

The interphase mass exchange factor  $\Delta c$  (the evaporation rate) can be written as follows:

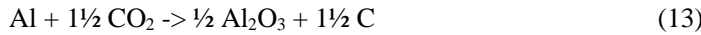
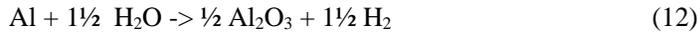
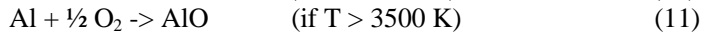
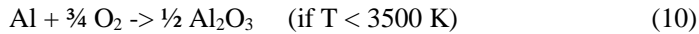
$$\Delta c = (3\phi_s \rho_s / \tau)(1 + 0.276\sqrt{Re}) \quad \text{for } T > T_{\text{ignition}} \quad (8)$$

where Re is a relative Reynolds number based on the particle diameter and velocity difference between the gas and solid phase.  $\tau$  is a characteristic time of combustion described as follows:

$$\tau = Kr, d_0^2 \quad (9)$$

where  $Kr$  is a burning rate constant and  $d_0$  is an initial diameter of particles.

To compute detailed chemical reaction models is infeasible, so 8 reactions and 10 species are considered in this study as follows:



The chemical reaction rates are obtained using infinite rate chemistry. This infinite reaction model is often used to model afterburn in HEs [4-9].

### 3 Computational and Experimental setup

To validate the developed numerical code, the numerical simulation of a blast evolution of a heavily aluminized (35% weight ratio (wt)) HE in a 26m<sup>3</sup> chamber was performed. The experiment was performed by DRDC Suffield in Canada [14]. The detailed experimental procedure was described in Ref. 13. In this reference, several weights of TNT with two types of Al particles, one was mixed into TNT and the other was shelled around TNT, were performed. From those experiments, the 4kg

TNT/Al (65%/35%wt) case was chosen in this study. The picture of the explosion chamber is shown in Fig. 1.

The Al particles used in this test was Valimet atomized H-30 Al with a mean diameter of 36  $\mu\text{m}$ . The charge shape was cylindrical, a length-diameter ratio was 0.83, and the charge density was 1.9 g/cc. The HE was put in the middle of the chamber and top-detonated. The chamber air pressure was brought to one standard atmosphere before the test.

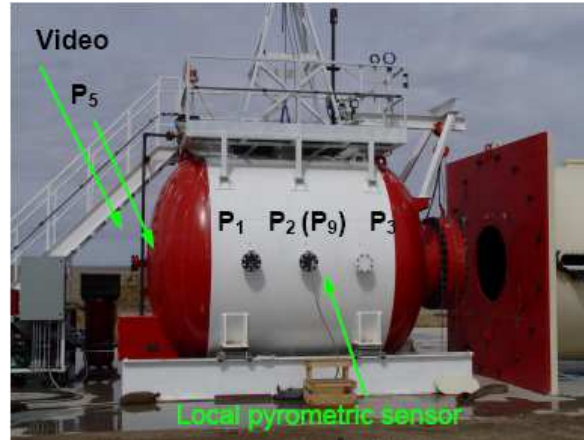


Figure 1: 26m<sup>3</sup> Explosion chamber and gauge locations

To save CPU time, the quarter size of the chamber was reproduced as the computational domain in Fig.2. A mesh resolution around the HE is very important to model the detonation initiation, so two computational domains with different mesh resolutions were prepared. One mesh has a 1mm computational cell size inside HE and 1cm resolution for farther area. The other has a uniformly 1cm cell size in whole domain.

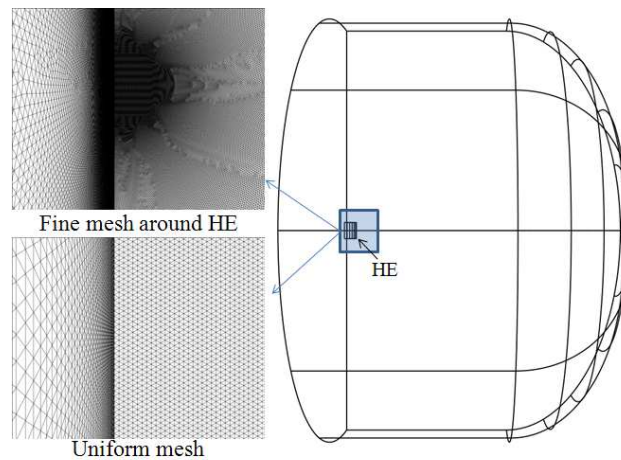


Figure 2: Computational domain and enlarged view of two different mesh resolutions around HE.

### 3 Computed results

The JWL EOS was used to model the detonation. The detonation species fraction of the initial condition was determined by the chemical software, Cheetah [15]. Cheetah is the chemical software developed by Lawrence Livermore National Laboratory (LLNL). One of the functions of Cheetah gives the detonation species mass fraction at various temperatures. The detonation species at frozen temperature (1800K) were used for the initial species, but given species were still too many, so

several important species (9 species described above) were chosen as initial species in this study. Figure 3 shows the absolute velocity Gouraud shading of the detonation initiation of the 4kg TNT/Al (65%/35% wt). The computed result was interpolated into the uniform cell size mesh after the detonation initiation finished.

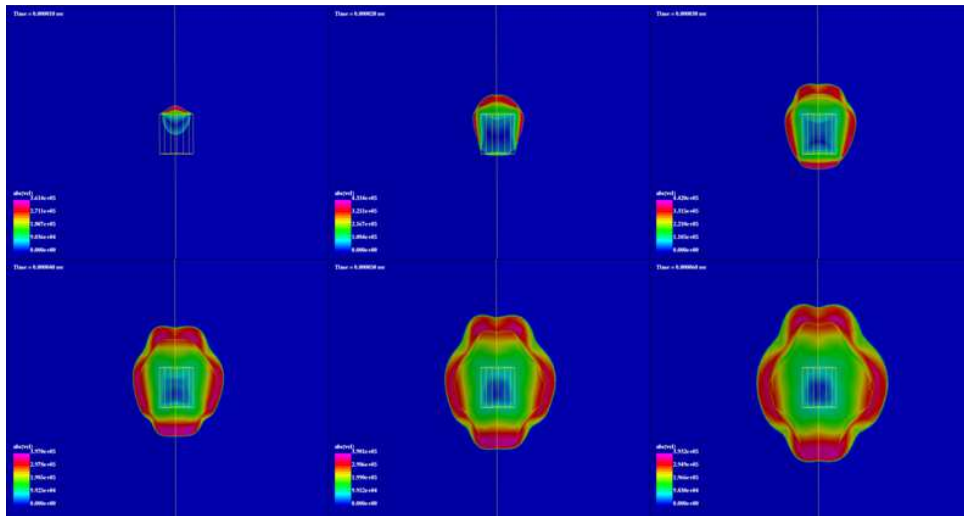
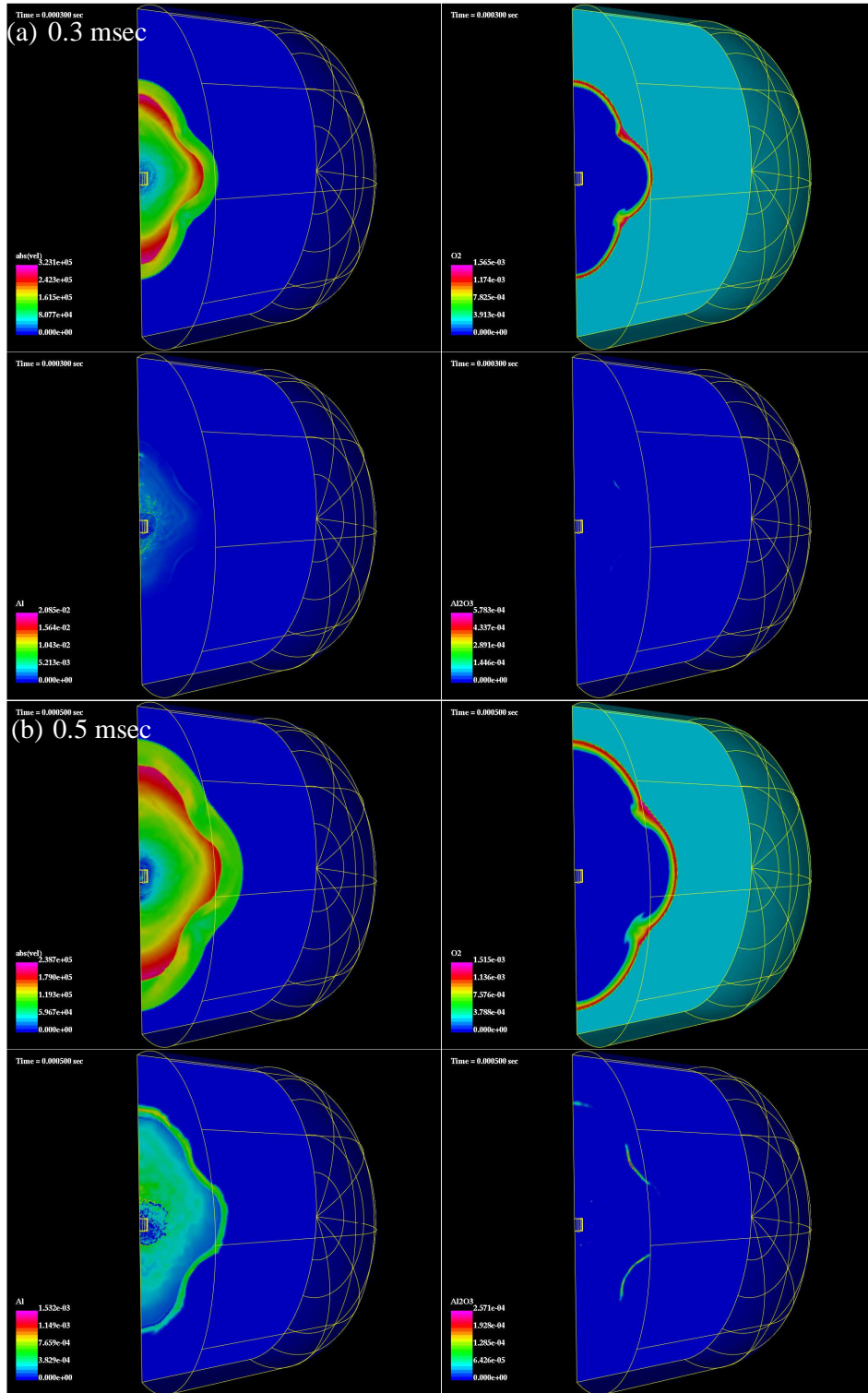
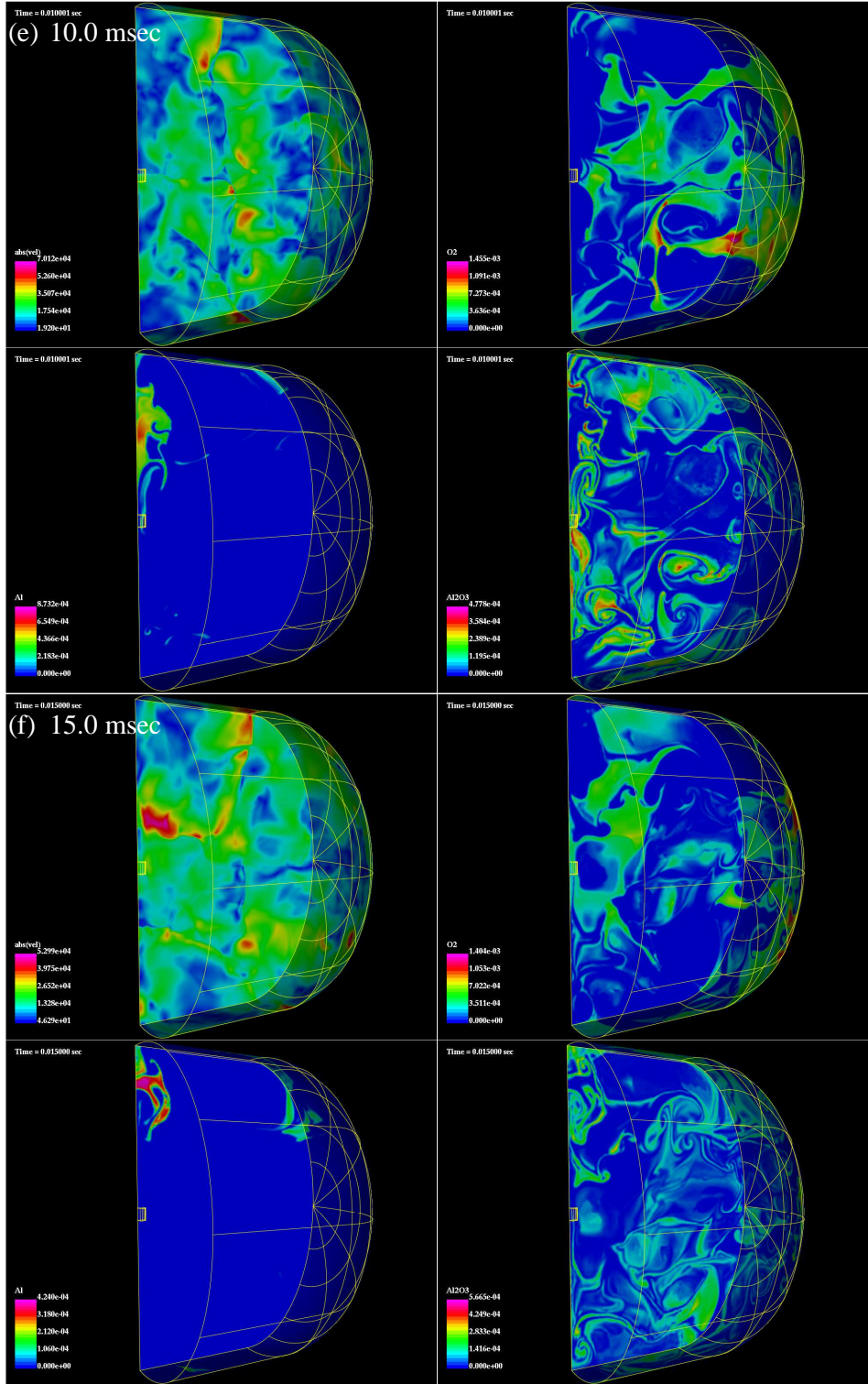


Figure 3: Computed detonation initiation of the 4kg TNT/Al (65%/35% wt) (Absolute velocity)

Figure 4 shows the Gouraud shadings of  $O_2$ , C, Al, and  $Al_2O_3$  densities. Oxygen was not contained as the detonation products, so there was no oxygen in Fig. 4 (a) and (b). Aluminum particles started evaporating in Fig. 4 (a) and they started reacting with the detonation products. Generated small amount of  $Al_2O_3$  were observed behind the blast wave in Fig. 4 (b). The blast wave reached chamber wall and the shock reflection enhanced the mixture among the ambient air and detonation products in Fig. 4 (c). Evaporated aluminum reacted with the ambient oxygen and generated  $Al_2O_3$ . The shock reflections were not symmetric because of the top detonation. The diffusion of  $Al_2O_3$  were also not symmetric in Fig. 4 (c) and (d). The evaporated aluminum, which was located at the spot with no oxygen,  $H_2O$ , nor  $CO_2$ , could not react and stayed in as aluminum itself in Fig. 4 (e) - (g), while there was a very tiny amount.







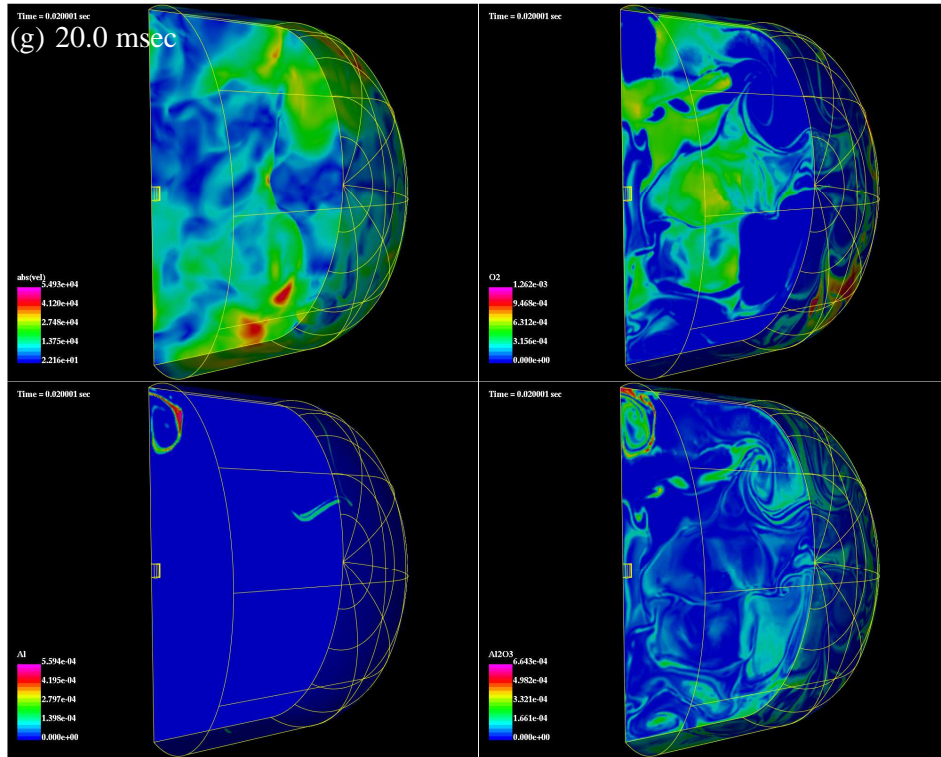


Figure 4: Computed Gouraud shadings of absolute velocity, O<sub>2</sub> density, Al density, Al<sub>2</sub>O<sub>3</sub> density at (a) 0.3 msec, (b) 0.5 msec, (c) 1.6 msec, (d) 5 msec, (e) 10 msec, (f) 15 msec, and (g) 20 msec

Figure 5 shows the comparison between experimental results and several computed results. The computations were performed using three different models; the new model, the Miller model, and no afterburn model. All computations used the JWL EOS for the detonation initiation. The computations were performed using quarter symmetric domain, so the pressure gauge P2 and P9 in Fig. 1 were compared with one computed station location, and so do the pressure gauge P1 and P3. The black line and blue line denotes the experimental data in Fig. 5. The magenta line denotes the computed result using the new model, the orange line denotes the computed result using the Miller model, and the cyan denotes the computed result with no afterburning model. All the computation used the JWL EOS, so they agreed very well with TOA of the incident and the second pressure peak. However, the computed result with no afterburning model shows clearly low impulse estimation, shortage of the energy release. The computed result using the Miller model shows higher impulse because the Miller model released the energy by the function of the pressure without considering the diameter of the particles and evaporating rate. The Miller model showed good agreement with an experimental data under the condition of a larger room with a smaller charge [3], but in the case of relatively smaller room such as in this study, or very close to the HE location, this model might estimate higher energy release. The computed result using the new model, which considered the initial diameter of the particle, the evaporating rate, and the chemical reaction, showed much better agreement with the experimental data, especially at the gauge P9. All the computed results showed larger pressure oscillation than the experiment. This less pressure oscillation might be caused by the dust in the chamber. Plenty of dust could diminish the shock propagation quickly. All the computation models do not consider the dust after reaction and resulted in the larger pressure oscillation.

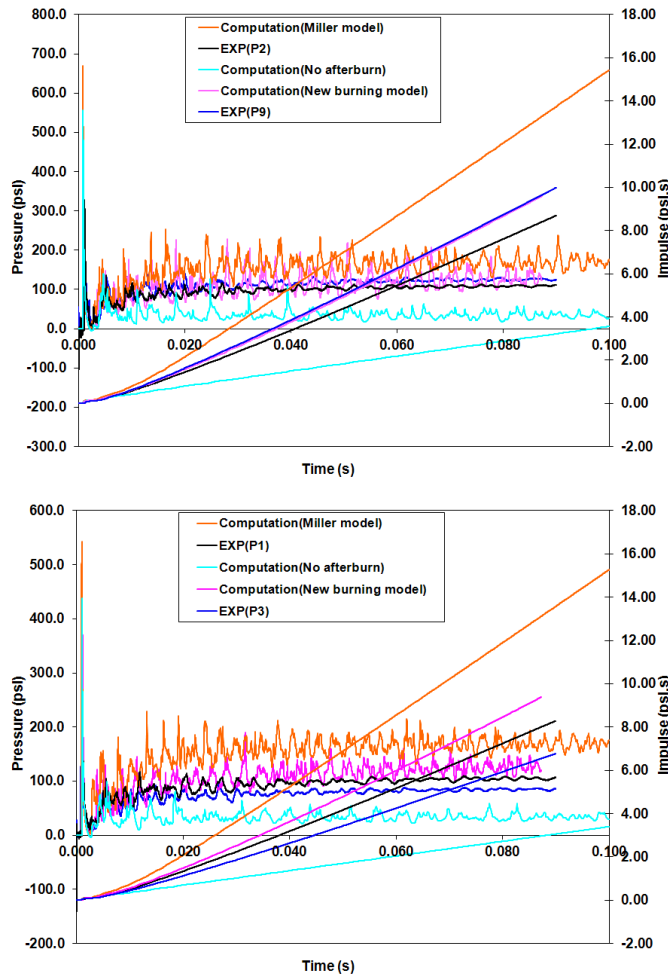


Figure 5: Pressure and Impulse history comparisons between the experimental data and computed results (black and blue: experimental data, magenta: computed result with the new model, orange: computed result using Miller model, cyan: computed result with no afterburn)

#### 4 Concluding remarks

The Numerical modeling of burning particles, initiated from a heavily aluminized High Explosive (HE) is being investigated. Reactive multiphase flows were modeled and incorporated into our in-house code, FEFLO. The new developed code was applied to the numerical simulation of the heavily aluminized HE (TNT/Al 65%/35% wt) explosion inside the explosive chamber. The computed result was compared with the experimental data and the computed result using the Miller afterburning model and the computed result with no afterburning model. The computed result using the new model showed good agreement with the experimental data. The comparison with another computed cases showed the significance of modeling the particle evaporating and chemical reaction especially when the HEs contained relatively large aluminum particles and were confined in a small room or cased condition. Consideration of dust generated by the detonation and the afterburn was also important to model correctly in such a situation.

#### References

- [1] P.C. Souers, Ben Wu, and L.C. Haselman, Jr., "Detonation Equation of State at LLNL, 1995," Energetic Materials Center Lawrence Livermore National Laboratory, February 1, 1996

- [2] P. J. Miller, "A Reactive Flow Model with Coupled Reaction Kinetics for Detonation and Combustion in Non-Ideal Explosives," MRS Proceedings, vol. 418, pp. 413, doi:10.1557/PROC-418-413, 1995
- [3] F. Togashi, J. D. Baum, E. Mestreau, R. Löhner, and D. Sunshine, "Numerical Simulation of Long-duration Blast Wave Evolution in Confined Facilities," *Shock Waves*, vol. 20 issue 5, 2010, pp.409-424
- [4] R. C. Ripley, L. Donahue, T. E. Dunbar and F. Zhang, "Explosion Performance of Aluminized TNT in a Chamber," Proc. 19<sup>th</sup> Military Aspects of Blast and Shock, Calgary, Canada, 2006
- [5] C.K. Kim, J.G. Moon, J.S. Hwang, M.C. Lai, and K.S. Im, "Afterburning of TNT Explosive Products in Air with Aluminum Particles," AIAA-2008-1029, 2008
- [6] K. Balakrishnan and S. Menon, "On the Role of Ambient Reactive Particles in the Mixing and Afterburn Behind Explosive Blast Waves," *Combust. Sci. and Tech.*, vol 182, pp.186-214, 2010
- [7] A. Khasainov, B. Veyssiere, "Steady, Plane, Double-front Detonations in Gaseous Detonable Mixtures Containing a Suspension of Aluminum Particles," *Dynamics of Explosions: Progress in Astronautics and Aeronautics* 114, AIAA, pp284-299, 1988.
- [8] A. L. Kuhl, R.E. Ferguson, and A.K. Oppenheim, "Gas dynamic model of turbulent exothermic fields in explosions," *Progress in Astronautics and Aeronautics Series*, 173, pp. 251-261, 1997
- [9] D. Schwer and K. Kailasanath, "Blast Mitigation by Water Mist (1) Simulation of Confined Blast Waves," NRL/MR/6410-02-8636.
- [10] I. A. Johnston, "The Noble-Abel equation of state: Thermodynamic derivations for ballistics modeling." *Defense Sci. Tech. Org.*, DSTO-TN-0670, 2005
- [11] Paul W. Cooper, and Stanley R. Kurowski, "Introduction to the Technology of Explosives," WILEY-VCH.
- [12] C.B. Henderson, "Drag Coefficients of Spheres in Continuum and Rarefied Flows," *AIAA J.* vol. 14, No. 6, pp. 707-708, 1976
- [13] D.J. Carlson and R.F. Hoglund, "Particle Drag and Heat Transfer in Rocket Nozzles," *AIAA J.* vol.14, No. 11, pp.1980-1984, 1964
- [14] F. Zhang, J. Anderson, and A. Yoshinaka, "Post-Detonation Energy Release from TNT-Aluminum Explosives," *Shock Compression of Condensed Matter 2007*, American Institute of Physics 978-0-7354-0469-4/07
- [15] L. E. Fried *et al.* "Cheetah 4.0 User's manual," LLNL, 2004